THE RESPONSE OF ORTHOTROPIC STEEL DECKS TO TRAFFIC LOADS

A. T. D E M P S E Y, D. L. K E O G H

DEPT OF CIVIL ENG., UNIVERSITY COLLEGE DUBLIN, IRELAND

and

B. J A C O B, J. C A R R A C I L L I

LCPC, PARIS, FRANCE

This paper describes the instrumentation and load testing of a three-span orthotropic steel bridge in France. Strain gauges were attached to the underside of the orthotropic plate to measure the dynamic response of the bridge to traffic loading. Two preweighed trucks were driven across the bridge at different velocities to investigate the influence of truck speed on the dynamic amplification of the bridge. A model suitable for the prediction of the dynamic response of the bridge is described. This consists of an elaborate finite element model to determine the natural frequencies and mode shapes of the bridge, and a dynamic model which uses this information to determine the dynamic response. The results of the experimentation are presented and the relationship between truck speed and dynamic amplification are shown. Finally, the loads applied to the bridge by an instrumented truck driving over it are presented and comparisons are made with the loads applied at the bridge approaches.

1. Introduction

Orthotropic steel deck bridges are characterised by the use of a longitudinally stiffened steel plate for the deck structure. The principal advantage of this form over a reinforced concrete slab is a reduction in the weight of the bridge. This becomes particularly important for long-span bridges and consequently orthotropic steel decks are regularly the favoured structural form for the decks of the world's longest bridges.

The word *orthotropic* is derived from *orthogonal* aniso*tropic* and means that the stiffness of the plate is different in the two orthogonal directions, namely the longitudinal and transverse directions. When such bridges were first designed in the 1930's in Germany (HEINS and FIRMAGE, [3]), they were used as moveable bridges as the weight of the bridge deck had to be less than that of the conventional reinforced concrete slab. Since then, orthotropic steel decks have become more widely used particularly in the deck construction of long span bridges, where the self-weight of the bridge becomes an important problem in the design process. As a result, the ratio of the live traffic loads to the dead weight of the bridge is greater for orthotropic bridges and consequently, they are more susceptible to fatigue damage from traffic loads. This paper examines the response of orthotropic steel decks to both static and dynamic truck loads. A comparison of the dynamic loads induced by an instrumented vehicle on a portion of road surface before the bridge and on the bridge is also examined.

2. INSTRUMENTATION AND EXPERIMENTS

The bridge, which was instrumented, was an orthotropic steel deck, known as Autreville bridge, located on the A31 motorway between Nancy and Metz, in Eastern France. The bridge consists of three spans (74.5 m, 92.5 m and 64.75 m) (Fig. 1). There are four lanes and two emergency lanes, which are carried by the steel plate of approximately 30.5 m in width. It has longitudinal stiffeners, which are trapezoidal in shape at 600 mm centres. The plate is supported every 4.62 m by transverse cross-beams, which span between the two main I-beams (3.8 m in height) of the bridge (Fig. 2). The instrumentation consists of strain gauges, which were placed in the longitudinal direction on the bottom of the longitudinal stiffeners (Figs. 3 and 4).
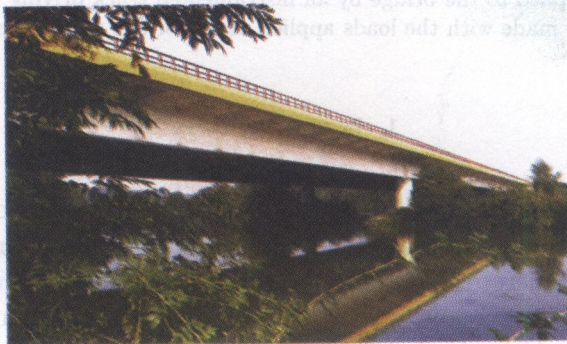

FIG. 1. Elevation of Autreville bridge.
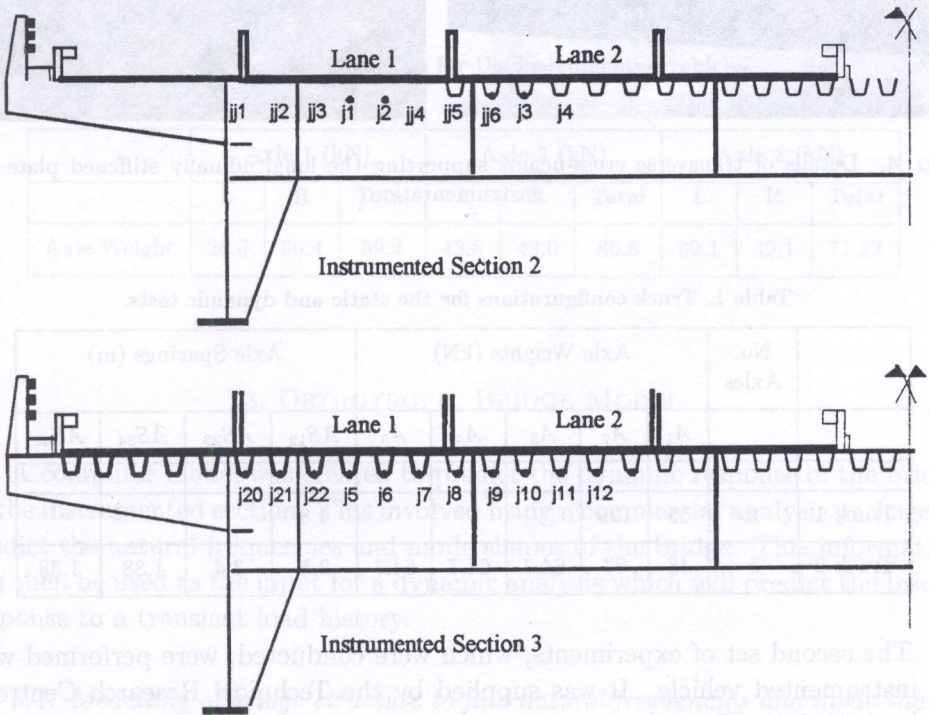
FIG. 2. Bridge structure.

FIG. 3. Schematic of instrumented sections 2 and 3.

Two different experiments are described in this paper. The first consists of comparing the dynamic response of the bridge to the passage of two different truck configurations to that of the quasi-static response of the bridge. The second series of tests consists of examining the bridge response to the passage of an instrumented truck. The two truck configurations, which were used in the first test, were a 2-axle rigid truck and a 5-axle semi-trailer. The axle weights and

spacings for the two vehicles are given in Table 1. Both of the trucks were driven across the bridge four times at each of the following velocities, 5, 10, 20, 30, 40, 50, 60 and 80 km/h, and the response of the bridge to each truck crossing was recorded at both instrumented sections.

FIG. 4. Details of transverse cross-beams supporting the longitudinally stiffened plate and instrumentation.

Table 1. Truck configurations for the static and dynamic tests.

	No. Axles	Axle Weights (kN)					Axle Spacings (m)			
		A_1	A_2	A_3	A_4	A_5	AS_{12}	AS_{23}	AS_{34}	AS_{45}
Truck 1	2	55	129				4.8			
Truck 2	5	48	87	64.7	64.7	64.7	3.5	3.4	1.38	1.38

The second set of experiments, which were conducted, were performed with an instrumented vehicle. It was supplied by the Technical Research Centre of Finland (VTT). The instrumented vehicle was a three-axle rigid vehicle, the second and third axle being a tandem. Traditional steel springs are used in all three-axles. There is a mechanical connection between the two axles on the tandem, which means the axle masses are not distributed equally within the tandem (55% and 45% of the tandem axle mass is carried by the first and second axle respectively). The technical details of the instrumented vehicle are presented in Table 2 (HUHTALA et al., [4]) and the exact wheel weights for the experiments conducted on the Autreville bridge are illustrated in Table 3.

Table 2. Technical details of the instrumented VTT truck.

Parameter	Axle 1	Axle 2	Axle 3
Maximum Weight (kN)	58.9	86.3	70.6
Axle Spacing (m)		4.2	1.2
Spring Stiffness (N/mm)	210	1600	
Body Bounce Freq. (Hz)	2.5	3	3
Axle Hop Freq. (Hz)	11	10	10

Table 3. Wheel weights for the instrumented vehicle.

	Axle 1 (kN)			Axle 2 (kN)			Axle 3 (kN)		
	L	R	Total	L	R	Total	L	R	Total
Axle Weight	28.0	30.4	59.4	43.8	43.0	86.8	32.1	39.1	71.22

3. ORTHOTROPIC BRIDGE MODEL

A computer model was created to predict the dynamic response of the bridge at the instrumented section. This involved using a commercial analysis package to predict the natural frequencies and mode shapes of the bridge. This information can then be used as the input for a dynamic analysis which will predict the bridge response to a transient load history.

3.1. Modelling of bridge structure to find natural frequencies and mode shapes

Modelling of orthotropic bridges requires greater effort than that of more conventional bridge types. As well as the complexities of the orthotropic behaviour, the relative flexibility of the plate between transverse beams introduces additional complexities. A combined grillage and finite element model was created using the structural analysis program STRAP (ATIR, [1]). This was analysed to predict the natural frequencies and mode shapes of the bridge. This information was then used in a dynamic model to predict the response of the bridge when subjected to the moving truck loads.

The choice of model type was arrived at by considering both the behaviour of the bridge and the predictions required, namely the natural frequencies and mode shapes. The longitudinal girders and transverse beams were modelled using a three-dimensional array of beams, or a '3d grillage'. This approach was chosen as it allowed direct modelling of the difference in location of the centroids of these members. Rigid (or very stiff) vertical beams were used to connect the longitudinal and transverse members at discrete locations. The orthotropic plate was modelled using plate finite elements. Once again, these were located at such a level that their centroids were coincident with the centroid of the plate. Rigid vertical beams connected these finite elements to the transverse beams at the appropriate locations. Figure 5(a) shows a view of the complete combined grillage and finite element model while Fig. 5(b) shows a small portion of this model indicating the important components. The specific issues relating to the various components of the model are discussed in the following sections.
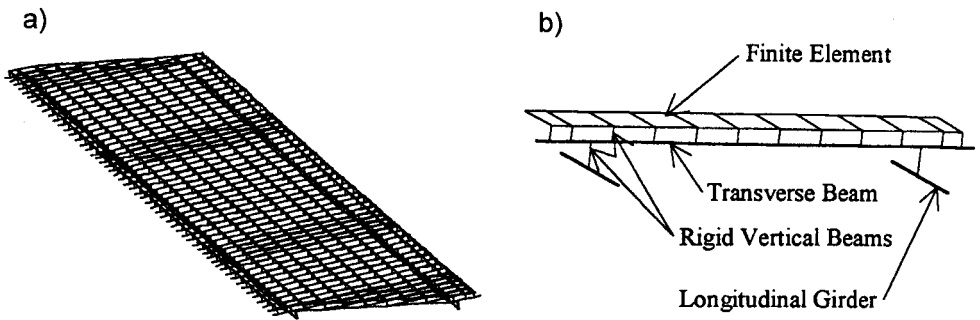

FIG. 5. (a) Combined grillage and finite element model; (b) Small portion of model.

3.2. Longitudinal girders

Although the depth of the girders is constant, the thickness of the bottom flange varies along the span resulting in a varying moment of inertia and a centroid of varying depth. To allow for this, each portion of the longitudinal girders were modelled at the level of their centroids and connected by rigid vertical members. The properties of the members in the model were derived from the web and bottom flange of the girders. The orthotropic plate forms the top flange of the girders and consequently, its stiffness was incorporated in the model by the finite elements. The moment of inertia of the members representing the girders was determined by considering the web and bottom flange bending about the centroid of the combined web and bottom flange section. The torsional constant was determined by adding the torsional constants of the rectangles of the web and bottom flange. WEST [7] describes this method in detail. As the model is

three-dimensional, it was necessary to assign the moment of inertia for transverse bending of the girders. Although being very small compared to that for longitudinal bending, it was considered important to determine this quantity accurately as it could affect some of the higher mode shapes.

The top flange of the girder is idealised using finite elements (which are capable of in-plane distortion). It was not necessary to consider shear lag as it is automatically modelled. This is one of the distinct advantages of using a three-dimensional model rather than attempting to estimate effective flange widths which will inevitably be affected by the type of loading applied to the bridge.

3.3. Transverse beams

The transverse beams, which were spaced at between 3.82 m and 4.62 m apart, were modelled in a similar manner to the longitudinal girders. One exception was that the beams have a top flange on which the orthotropic plate rests. The beams were modelled at the level of their centroids which was above the centroid of the longitudinal girders and below the centroid of the orthotropic plate. Consequently two sets of rigid vertical beams were required, one to connect to the girders and one to connect to the plate. The transverse beams run perpendicularly to the span direction and were modelled accordingly. Skew transverse beams are located at the two ends of the bridge. These were also modelled and connected to the longitudinal girders and plate by rigid vertical members.

3.4. Orthotropic plate

The orthotropic plate is perhaps the most challenging part of the bridge to model correctly. It was decided to use orthotropic finite elements to this end. The plate on the bridge is 'geometrically orthotropic' as it is its geometry that gives it different stiffnesses in the longitudinal and transverse directions. It is made of one homogenous material, namely steel, which gives it the same material properties in all directions. Most commercial finite element programs do not incorporate elements which allow for modelling of this type of plate directly. Alternatively, they use 'materially orthotropic' elements. These assume the same stiffness in both orthogonal directions by adopting a single thickness for the plate. The orthotropy is accounted for by allowing the specification of different moduli of elasticity in the two directions. As the stiffness of the plate is a function of the product of moment of inertia and modulus of elasticity, EI, by adjusting the value of E in the two directions the difference in moments of inertia can be allowed for.

Since the main aim of this model was to determine the natural frequencies of the bridge, it is important that the weight of the model should be accurate as well as the stiffness. For this reason, the depth of the elements was chosen so as to give the correct cross-sectional area of the plate (and hence correct weight) and the modulus of elasticity in both the longitudinal and transverse directions were adjusted to give the correct EI values (and hence correct stiffness). Further information on this technique is given in O'BRIEN and KEOGH [5].

In order to check the validity of the chosen technique for modelling the orthotropic plate, especially with regard to predicting its natural frequencies, a small portion of plate was considered in isolation. A geometrically orthotropic finite element model was generated using a three-dimensional assemblage of isotropic elements for a 6 m square plate. Figure 6 shows a picture of a portion of this model. The dimensions of this plate correspond to those of the actual bridge. The plate was fixed against all translations and rotations at all of its edges. A materially orthotropic finite element model of this plate was also analysed with the same boundary conditions. Comparisons were made between the first five natural frequencies predicted by the two models. These are shown in Table 4. The maximum deflection of the plate under the action of a 10 kN/m^2 uniform load was also compared. This is also shown in the table.
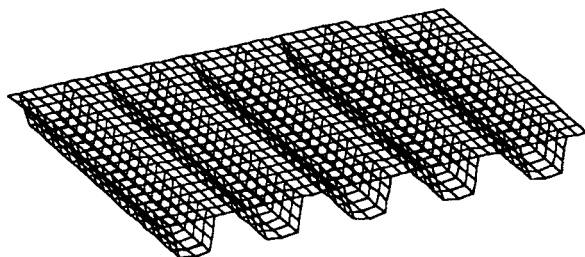

FIG. 6. Portion of geometrically orthotropic finite element model.

Table 4. Natural frequencies and deflection for 6m square orthotropic plate models.

Model Type	First Mode (Hz)	Second Mode (Hz)	Third Mode (Hz)	Fourth Mode (Hz)	Fifth Mode (Hz)	Maximum Deflection (mm)
Geometrically Orthotropic	43.44	46.62	51.65	57.72	64.39	1.22
Materially Orthotropic	44.61	45.85	48.02	51.27	55.73	1.12
% Variation	2.7	1.7	7.0	11.2	13.5	8.2

As the natural frequencies are predicted reasonably well by the materially orthotropic finite element model of the 6m square plate, particularly for the lower modes, it was considered sufficiently accurate to be used for the model of the full bridge. Great care was taken to ensure the correct weight of the bridge was used in the model. The weight of road surfacing was included as this accounted for approximately 30% of the weight of the bridge. This is a particular feature of long-span steel orthotropic bridges. A final check was made by comparing the weight of the model with the known weight of the bridge as determined by its designers and constructors.

3.5. Calculation of modes and natural frequencies

The model of the bridge was analysed to determine the first 150 natural frequencies. This gave all of the mode shapes up to a frequency of over 25 hertz. This was taken as the highest frequency likely to be excited by the moving trucks. Although a large number of mode shapes were considered, only a small number of these are significant in determining the dynamic response of the instrumented section of the bridge. Typically these might be the first several modes of the entire bridge and the modes of local bending of the orthotropic plate between transverse beams at the instrumented section.
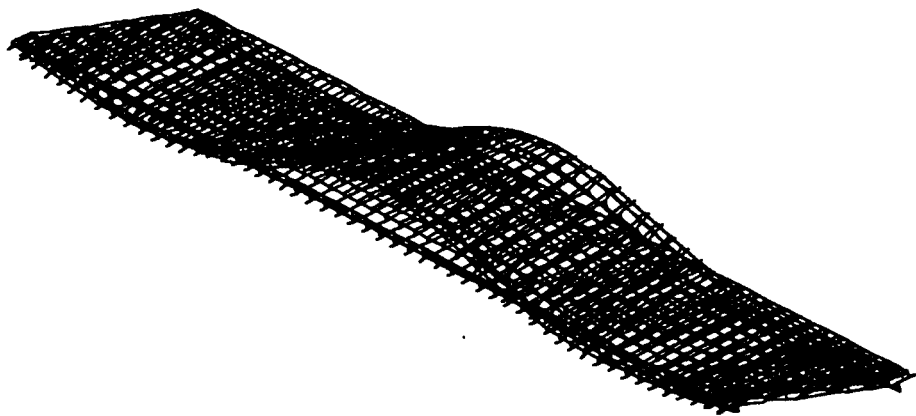

FIG. 7. First mode shape of bridge.

The density of the finite element mesh was increased locally in the region corresponding to the instrumented section. This was done to provide greater accuracy for localised mode shapes in this region. It was not practical to provide such a fine mesh density throughout the model due to excessive analysis times, nor was it considered necessary as the results were only required for the instrumented

section in this case. Figure 7 shows a plot of the first mode shape of the bridge. This corresponds to a frequency of 1.07 hertz. Figure 8 shows mode shape number 150 which shows a localised vibration in the region of the instrumented section. This corresponds to a frequency of 26.48 hertz. Table 5 shows the frequencies of the first 50 mode shapes.
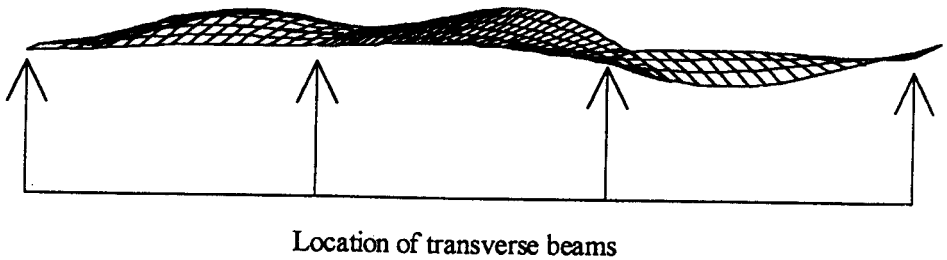

Location of transverse beams

FIG. 8. 150th mode shape (elevation), localised vibration of instrumented section.

Table 5. First 50 natural frequencies of bridge.

mode	F (Hz)	mode	F (Hz)	mode	F (Hz)	mode	F (Hz)	mode	F (Hz)
1	1.0732	11	4.1836	21	5.896	31	7.0003	41	8.4743
2	1.278	12	4.4658	22	5.9859	32	7.2242	42	8.5733
3	1.5309	13	4.6063	23	6.0551	33	7.2757	43	9.0462
4	1.7475	14	4.767	24	6.1271	34	7.3263	44	9.216
5	2.0127	15	4.8871	25	6.2238	35	7.5749	45	9.5807
6	2.2071	16	5.0448	26	6.3242	36	7.6932	46	9.7779
7	2.7669	17	5.4	27	6.5078	37	7.8172	47	9.9099
8	3.0954	18	5.5026	28	6.7029	38	7.9217	48	10.0005
9	3.3628	19	5.6867	29	6.7499	39	8.142	49	10.3955
10	3.9365	20	5.8295	30	6.9278	40	8.3093	50	10.5789

3.6. Calculation of transient bridge response

The general equation of motion of the bridge is expressed as:

$$(3.1) \qquad [\mathbf{M}]\ddot{\mathbf{x}} + [\mathbf{C}]\dot{\mathbf{x}} + [\mathbf{K}]\mathbf{x} = F(t)$$

where $\mathbf{x}$ is the nodal displacement vector, $[\mathbf{M}]$ the mass matrix, $[\mathbf{C}]$ the damping matrix, $[\mathbf{K}]$ the stiffness matrix, and $F(t)$ the force(s) applied to the structure as a function of time.

If the model contains m nodes, there are m degrees of freedom, i.e., m sets of displacements. Equation (3.1) becomes difficult to solve as the $[\mathbf{M}]$, $[\mathbf{C}]$ and $[\mathbf{K}]$ matrices cause coupling in the system. Therefore, the process of modal decoupling

is used. This is the process by which the modes of vibration of a structure are used to reduce a multi-degree of freedom system to obtain the equations of motion in terms of just one-degree of freedom systems. The displacement vector $\mathbf{x}$, expressed in geometric co-ordinates, is transformed to generalised co-ordinates z, as

(3.2) $$\mathbf{x} = \phi z$$

where $\phi = \{\phi_1, \phi_2, ..., \phi_n\}$ is the matrix of the eigenvectors (mode shapes) and n is the number of modes used in the analysis. By substituting Eq. (3.2) into (3.1), pre-multiplying by ϕ^T (the transpose of the eigenvectors) and by taking advantage of the orthogonality properties (CLOUGH and PENZIEN, [2]) of the eigenvector relative to the mass and stiffness matrices, we obtain:

(3.3) $$\phi^T[\mathbf{M}]\phi = \begin{bmatrix} 1 & 0 & 0 & 0 \\ 0 & 1 & 0 & 0 \\ 0 & 0 & . & . \\ 0 & 0 & . & 1 \end{bmatrix}$$

(3.4) $$\phi^T[\mathbf{K}]\phi = \begin{bmatrix} \omega_1^2 & 0 & 0 & 0 \\ 0 & \omega_2^2 & 0 & 0 \\ 0 & 0 & . & . \\ 0 & 0 & . & \omega_n^2 \end{bmatrix}$$

However, decoupling the damping matrix $[\mathbf{C}]$ can only occur if it is assumed that the corresponding orthogonality condition applies to the damping matrix:

$$\phi^T[\mathbf{C}]\phi_i = 0, \qquad m \neq i,$$

(3.5)

$$C_i = \phi_i^T[\mathbf{C}]\phi_i = 2\xi_i\omega_i,$$

where i is the i-th degree of freedom, ω_i is the i-th natural frequency and ξ_i is the modal damping ratio of the i-th mode.

In this derivation of the normal co-ordinates equations of motion, it has been assumed that the normal co-ordinate transformation serves to uncouple the damping forces in the same way as it uncouples the inertia and elastic forces. However, there are only certain conditions under which this decoupling will occur. Rayleigh damping assumes that the damping matrix can be expressed in terms of the stiffness and mass matrix as follows:

(3.6) $$[\mathbf{C}] = a_0[\mathbf{M}] + a_1[\mathbf{K}]$$

where a_0 and a_1 are arbitrary proportionality factors.

If Rayleigh damping is used, the damping matrix satisfies the orthogonality conditions and therefore it can be decoupled. Therefore, it is evident that a damping matrix proportional to the mass and/or stiffness matrix will enable uncoupling of the equations of motion. With this type of damping matrix it is possible to compute the damping influence coefficients necessary to provide a decoupled system having any desired damping ratio in any specified number of modes (CLOUGH and PENZIEN, [2]). For each mode i, the generalised damping is given by :

$$(3.7) \qquad\qquad C_i = \phi_i^T[\mathbf{C}]\phi_i = 2\xi_i\omega_i.$$

Therefore, the set of equations described in (3.1) becomes:

$$(3.8) \qquad\qquad \ddot{z}_i + 2\xi_i\omega_i\dot{z}_i + \omega_i^2 z_i = R(t); \qquad i = 1, 2, ..., n$$

where n is the number of degrees of freedoms, and $R(t)$ is called the response function which is defined as the generalised force associated with mode n and is defined as:

$$(3.9) \qquad\qquad R(t) = (\phi^T)(F(t)).$$

The natural frequencies of bridges can readily be calculated by analytical methods or by experiment. However, as the evaluation of a specific damping property is impracticable, the damping is generally expressed in terms of damping ratios established from experiments on similar structures (CLOUGH and PENZIEN [2]).

Equation (3.8), which is a second order differential equation, can be solved to calculate the generalised displacements for each mode shape by using the Runge-Kutta method in which the second order equation is divided into two first order equations (THOMSON, [6]). The calculation of the dynamic displacements then follows a simple recursive method:

1) Firstly, a load or train of loads, i.e., a vehicle, is placed at the beginning of the bridge, with initial conditions of zero bridge displacement, velocity and acceleration. The acceleration of the bridge is assumed to vary linearly between the initial position and the first time step.

2) At any time increment $(t + \Delta t)$, the longitudinal position of a load or vehicle is determined.

3) The response function of the bridge is then determined for the particular longitudinal position. This is done by geometrically apportioning the loads to the four closest nodes and multiplying the nodal forces by the nodal mode shape ordinates.
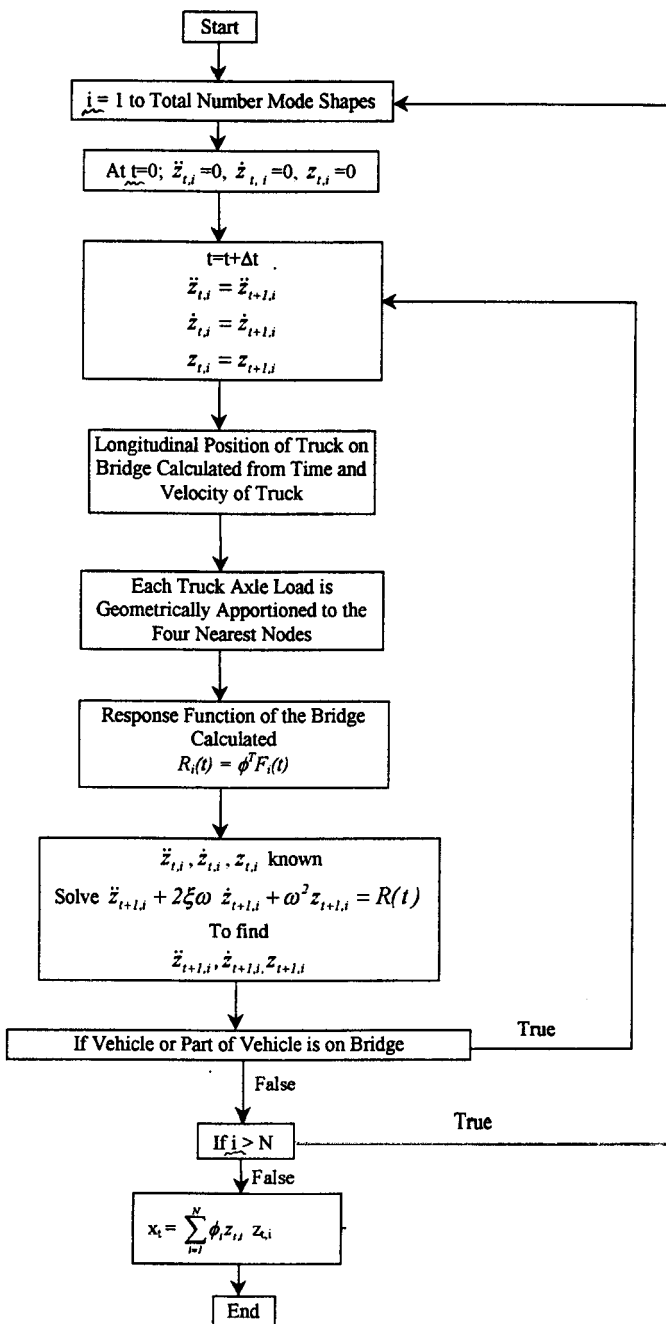
Start

$i = 1$ to Total Number Mode Shapes

At $t=0$; $\ddot{z}_{t,i}=0$, $\dot{z}_{t,i}=0$, $z_{t,i}=0$

$t=t+\Delta t$
$\ddot{z}_{t,i} = \ddot{z}_{t+1,i}$
$\dot{z}_{t,i} = \dot{z}_{t+1,i}$
$z_{t,i} = z_{t+1,i}$

Longitudinal Position of Truck on Bridge Calculated from Time and Velocity of Truck

Each Truck Axle Load is Geometrically Apportioned to the Four Nearest Nodes

Response Function of the Bridge Calculated
$R_i(t) = \phi^T F_i(t)$

$\ddot{z}_{t,i}, \dot{z}_{t,i}, z_{t,i}$ known
Solve $\ddot{z}_{t+1,i} + 2\xi\omega\,\dot{z}_{t+1,i} + \omega^2 z_{t+1,i} = R(t)$
To find
$\ddot{z}_{t+1,i}, \dot{z}_{t+1,i}, z_{t+1,i}$

If Vehicle or Part of Vehicle is on Bridge — True

False

If $i > N$ — True

False

$x_t = \sum_{i=1}^{N} \phi_i z_{t,i}\ z_{t,i}$

End

FIG. 9. Flowchart for dynamic bridge model.

4) The displacement, velocity and acceleration of the bridge are known at this time step from calculations in the previous time step. These are input into the differential equation and the displacement, velocity and acceleration of the bridge are calculated for this time and the next time step.

5) The process is repeated until the load or vehicle clears the bridge and for each mode shape.

This procedure is illustrated in Fig. 9. Equation (3.2) is used to convert the generalised displacements to actual displacements for each mode shape. The total displacement of the bridge at any point of the bridge is the sum of the actual displacements for the individual mode shapes.

Once the transient response of the bridge has been found, this can be compared with the observed response of the bridge. This is the subject of ongoing research. Some of the experimental observations are presented and discussed in the next section of the paper.

4. Experimental results

This section discusses the results obtained from the two tests described earlier, namely the static and dynamic tests with the two different truck configurations.

4.1. Static and dynamic tests

The strain recorded on the underside of each of the seven longitudinal stiffeners located under the slow lane were summed to get the response at the section to the passage of both truck configurations. This was carried out for both instrumented sections. This procedure was repeated for all of the different truck velocities. Figure 10 shows the response of section 2 to the passage of the 2-axle rigid truck at two different velocities. These two velocities are 10 km/h and 80 km/h and induce the greatest and least amplitude of bridge response respectively. Figure 11 illustrates that this phenomenon, i.e, a reduction in the amplitude of bridge response with the increase of velocity was also found to be true for the 5-axle truck. However, this experimental relationship between bridge response and velocity is quite complex as illustrated in Fig. 12. This graph illustrates the dynamic amplification factors, DAF, of the bridge for different passages of the two trucks.

The DAF is calculated by dividing the response of the bridge due to a truck travelling at a certain velocity divided by the static response of the bridge. In this experiment, the quasi-static response (i.e. truck moving very slowly) of the bridge is used as the static response in the calculation of the DAF. It is evident

from Fig. 12, that the dynamic response of the bridge increases with increasing velocity up to a velocity of about 10 km/h. After 10 km/h, the response of the bridge begins to decrease steadily with increasing speed. The response of the bridge to a truck travelling at 80 km/h is 20% less than that due to a truck moving very slowly across the bridge. It was also found that the response of the bridge was similar for two completely different truck configurations. In fact, the DAF recorded at section 2, were almost identical for the two different truck configurations.
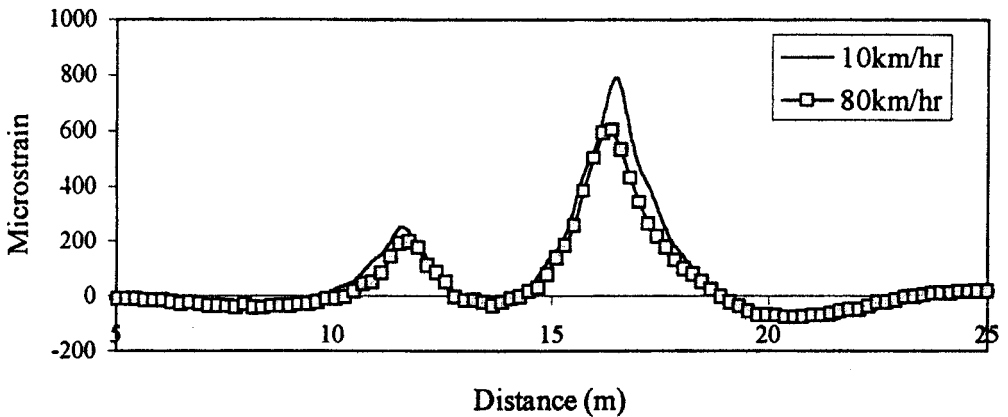
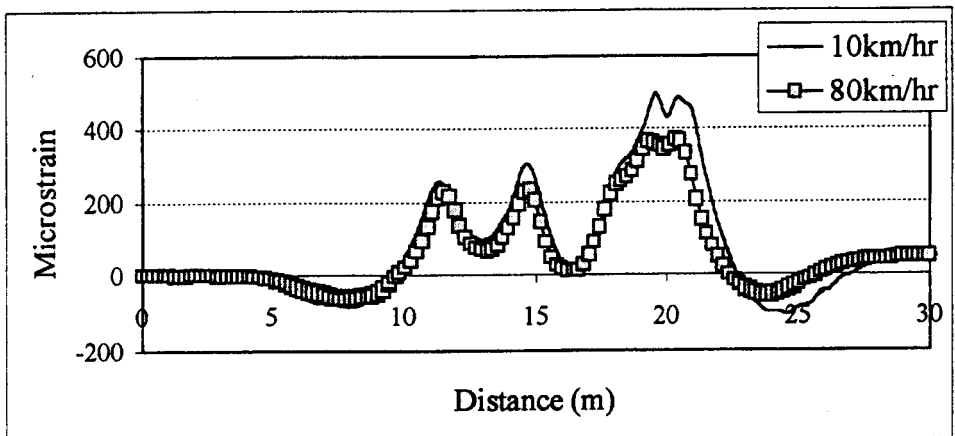FIG. 10. Response of orthotropic deck to 2-axle rigid truck at different velocities (section 2).

FIG. 11. Response of orthotropic deck to 5-axle semi-trailor at different velocities (section 2).
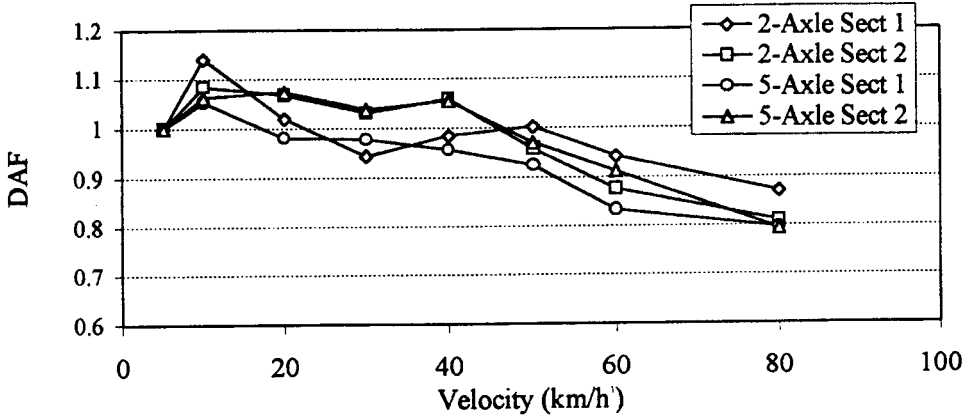
FIG. 12. Dynamic amplification factors.

4.2. VTT instrumented truck

One of the primary objectives of the experiment with the VTT instrumented truck was to compare the dynamic loads induced by the truck on a smooth road pavement and on the orthotropic deck. Figure 13 shows the variation of the dynamic axle weights of the first axle of the instrumented truck both on the pavement (Fig. 13a) and on the bridge (Fig. 13b). In order to achieve this comparison, these maximum and minimum impact factors (IF), (which are described as the dynamic axle load divided by the static axle load) for each of the axles were calculated for 4 runs of the instrumented truck on the smooth road pavement.
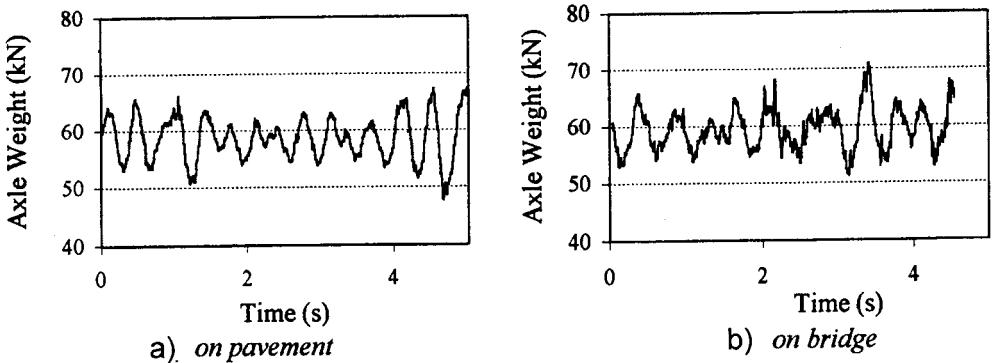

a) on pavement   b) on bridge

FIG. 13. Dynamic loads (1st axle) of VTT instrumented truck.

The average maximum and minimum IFs were then calculated. The same IFs were calculated for the truck on the bridge. Table 6 illustrates the comparison of the IFs for the truck on the pavement and on the bridge.

**Table 6. Average impact factors of axle loads for instrumented vehicle
(LW – Left Wheel, RW – Right Wheel).**

	1st Axle		2nd Axle		3rd Axle	
	LW	RW	LW	RW	LW	RW
IF (Pavement)	±21.9	±19.1	±33.6	±31.9	±36.1	±34.5
IF (Pavement)	±20.5		±32.7		±35.3	
IF (Bridge)	±19.3	±17.6	±29.5	±28.4	±39.1	±33.7
IF (Bridge)	±18.5		±28.9		±36.4	

It is evident from these results that the IFs of the truck on the bridge and on the pavement are quite similar. This is an interesting result, since generally the pavement is considered to be rigid when compared to the flexibility of a bridge. Therefore, the motion of the bridge could induce some motion in the truck. However, as can be seen from Table 1, it does not increase the maximum weight applied to the bridge by the truck in this case.
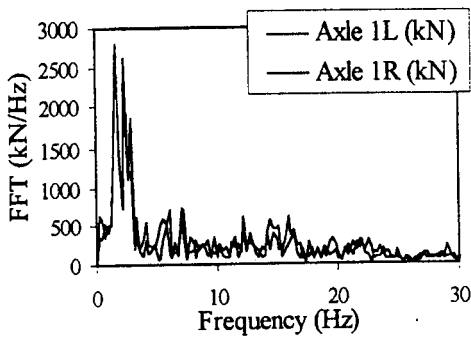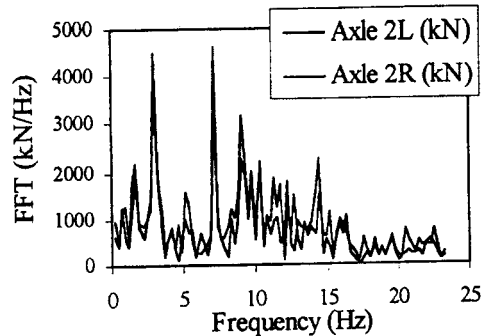
(a) *Front axle*   (b) *First axle of rear tandem*

FIG. 14. Frequency spectrum of dynamic axle loads.

A fast Fourier analysis (FFT) was also conducted on the dynamic axle loads and it was found that truck is vibrating at similar frequencies when it is travelling on the road pavement and on the bridge. Figure 14 illustrates the FFTs for the first and second axle of the instrumented truck travelling across the bridge. Figure 14(a) illustrates that the first axle is mainly vibrating at the body bounce frequency of the truck (2 – 3 Hz), while the vibration of the first axle of the

tandem is more complex, with frequencies of body bounce and axle hop (2 – 3 Hz and 10 Hz). The first harmonic of the out of roundness of the wheel can be clearly identified at 7 Hz also.

5. CONCLUSIONS

This paper describes the ongoing research project in which the behaviour of orthotropic steel deck bridges subject to static and dynamic vehicle loads is examined. Such a bridge has been instrumented in Eastern France and several experiments have been conducted. The two experiments described in this paper were devised to calculate the effect of speed on the response of the bridge and to compare the dynamic axle loads induced by an instrumented vehicle on the bridge and on a portion of road pavement adjacent to the bridge. The experiments are also being used to validate a dynamic orthotropic deck model, which is currently under development. The model consists of two parts, firstly a 3-D finite element and grillage model to calculate the natural frequencies and mode shapes of the bridge (recommendations are given on how to model the plate orthotropy) and secondly an analysis to calculate the dynamic transient response of the bridge subject to moving loads, by the method of modal superposition.

There were a number of significant results found from the experiments. Firstly, it was observed that the dynamic amplification factors (DAFs) were found to increase with increasing truck speed up to 10 km/h. After this, the DAFs started to reduce with increasing speed. It was found that the DAF was 20% less at 80 km/h than that at 5 km/h. This is an interesting finding for this particular type of bridge, as fatigue cracks normally occur in the weld between the longitudinal stiffener and the plate, which is close to the strain measurement point. The response of the bridge has been shown to be less for trucks travelling at normal highway speeds when compared to the static response. Therefore the fatigue damage would be less than that calculated with the static response of the bridge, which is the current procedure for fatigue assessment of such bridges. Another interesting finding is that the dynamic loads induced by the instrumented vehicle were the same on the road and on the bridge.

These findings could have implications on the methods and techniques that are used to assess orthotropic steel bridges for fatigue. However, these are experimental results from only one bridge. In order to validate, these findings, the model results will be compared to the experimental results. It is also the opinion of the authors that another experiment should be conducted on a similar bridge to validate the findings from the Autreville bridge.

REFERENCES

1. Atir, *STRAP, Structural Analysis programs user's manual version 6.00*, ATIR Engineering Software Development Ltd., Tel Aviv 1991.

2. R. W. CLOUGH and J. PENZIEN, *Dynamics of structures*, 2nd edition, Mc Graw Hill 1993.

3. C. P. HEINS and D. A. FIRMAGE, *Design of modern steel highway bridges*, John Wiley and Sons, New York 1979.

4. M. HUHTALA, P. HALONEN and V. MIETTINEN, *Cold environmental test at Lulea; Calibration of WIM systems using an instrumented vehicle*, Pre-Proceedings of the Second European Conference on Weigh-in-Motion of Road Vehicles, 409–417, B. JACOB and E. J. O'BRIEN, LISBON [Eds.], September, 1998.

5. E. J. O'BRIEN and D. L. KEOGH, *Bridge deck analysis*, E&FN Spon, London 1999.

6. W. T. THOMSON, *Vibrations of structures*, 4th ed., Chapman and Hall, London 1993.

7. R. WEST, *C&CA / CIRIA recommendations on the use of grillage analysis for slab and pseudo-slab bridge decks*, Cement and Concrete Association, London 1973.